AN INVESTIGATION OF THE INFLUENCE OF SCALING LAWS ON THE RATIO OF NEUTRON-PROTON CHARGE FORM FACTOR CALCULATIONS

Joseph Homer Brooks

United States
Naval Postgraduate School

THESIS

AN INVESTIGATION OF THE INFLUENCE OF SCALING
LAWS ON THE RATIO OF NEUTRON-PROTON
CHARGE FORM FACTOR CALCULATIONS

by

Joseph Homer Brooks
and
Gregg Frederick Sessler

Thesis Advisor: Franz A. Bumiller

June 1971

An Investigation of the Influence of Scaling Laws on the Ratio of Neutron-Proton Charge Form Factor Calculations

by

Joseph Homer Brooks
Major, United States Army
B.S., Jacksonville State College, 1961

and

Gregg Frederick Sessler
Ensign, United States Navy
B.S., United States Naval Academy, 1970

Submitted in partial fulfillment of the
requirements for the degree

MASTER OF SCIENCE IN PHYSICS

from the

NAVAL POSTGRADUATE SCHOOL
June 1971

ABSTRACT

An investigation of conventional and broken-symmetry scaling, and their effect on the ratio of the neutron-proton electric form factors, G_{En}/G_{Ep}, was carried out using measurements from elastic electron-deuteron and electron-proton scattering in the range of momentum transfers, q^2, of $0.10 \leq q^2 \leq 0.80\ F^{-2}$, and electron scattering angles of 45^{o} to 120^{o}. Within experimental errors of available data in this range of momentum transfers and angles, it was concluded that both forms of scaling as applied to the deuteron form factor have negigible effect on the ratio G_{En}/G_{Ep}, and the application of either scaling law to the proton form factor results in nearly identical corrections to this ratio, thus allowing no distinction between them, and the agreement of the experimental data with the neutron-electron interaction slope at $q^2 \simeq 0$ is not influenced by the choice of scaling law. A conclusive test for the scaling laws would require an improvement in experimental accuracy by at least an order of magnitude, a technically nearly impossible requirement.

TABLE OF CONTENTS

LIST OF TABLES

LIST OF FIGURES

I. INTRODUCTION

The elastic scattering of electrons by protons is described in the first Born approximation by the Rosenbluth equation [1]. In this approximation a single virtual photon is exchanged between the electron and the proton and the structure of the proton is represented by two electromagnetic form factors which are functions of q^2, the square of the four-momentum transferred by the virtual photon [2]. Janssens, et.al., [3] made absolute measurements of the elastic electron-proton cross sections with an accuracy of about 4% in the q^2 range from 4.0 to 30.0 F^{-2}(1 F = 1 Fermi = 10^{-15}m). These measurements verified the Rosenbluth equation for values of q^2 up to 22.0 F^{-2}, and determined the form factors of the proton to a precision exceeding that obtained in previous experiments. It was also found that the charge and magnetic form factors of the proton have the same dependence on q^2 within the accuracy with which they were determined.

Hundreds of other elastic electron-nucleon scattering measurements are also available, extending over a very wide range of q^2 and angle [4]. Empirically, the data seem to exhibit remarkable simplicity, the electric and magnetic form factors of nucleons obeying the "scaling law";

$$G_{Ep}(q^2) = \frac{G_{Mp}(q^2)}{\mu_p} = \frac{G_{Mn}(q^2)}{\mu_n} \equiv G_{SL};\ G_{En}(q^2) = 0 \qquad (1)$$

with the q^2 dependence being well described by the "dipole fit";

$$G_{SL} \simeq G_{Dipole} \equiv \frac{1}{(1 + q^2/M_D^2)^2} \qquad (2)$$

where $M_D^2 = 90.25\ F^{-2}$. It has long been clear that the electron-proton data show systematic oscillations about the dipole fit [5,6], but the amplitude seems to vary with laboratory and (2) is regarded as a remarkably good phenomenological fit.

Following the same general procedure as Rosenbluth did with the proton, Jankus [7] derived the cross section for the elastic electron-deuteron (e-d) scattering from a point deuteron in the first Born approximation. His results differ qualitatively from the proton cross section in one important way, i.e., there are three form factors characterizing the deuteron while two suffice for the proton. This is in agreement with the work of Glaser and Jaksic [8]. Their study showed that the cross section for the scattering of a relativistic electron from a potential with spin J contains 2J + 1 form factors. The three deuteron form factors correspond to the charge, quadrupole, and magnetic moments in the static limit $q^2 \to 0$. Dricker and Hand [9] experimentally verified for the deuteron an emperical relation between the form factors which is analogous to that for the proton. The scaling law for the deuteron may be written;

$$G_{ED} \simeq \frac{G_{MD}}{\mu'_D}\ , \quad \mu'_D = 1.71 = \frac{M_D}{M_p}\mu_D \ . \qquad (3)$$

Based on these scaling laws, Stewart [10] in a study of the neutron charge from factors at very low momentum transfers, found

that:

(a) The Feshbach-Lomon wave functions [11], together with relativistic corrections, removed an apparent discrepancy between the neutron-electron interaction slope at $q^2 \simeq 0$, and the slope given from values of G_{En} (obtained by electron scattering) in the range $0.10 \leq q^2 \leq 0.80\ F^{-2}$.

(b) Within the relatively large errors propagated into G_{En}, the Partovi wave functions [12] with relativistic corrections applied, are in disagreement with the neutron-electron interaction slope.

The important conclusion from Stewart's experimental results is that the neutron has a non-zero charge form factor, implying a charge distribution within the neutron.

Schumacher [4] however, points out that the theoretical situation is not satisfactory. The scaling law (1) led to the invention [13] of the phenomenlogical symmetry now called $SU(6)_W$, but a deeper interpretation appears to be lacking. Likewise, the dipole formula (2) corresponds to a double pole of mass 843 MeV instead of a combination of single poles at masses of realistic vector mesons. Although it was hoped that the oscillations around (2) might be explainable in dynamical terms, Goitein, Dunning and Wilson [5] showed that existing theories were not adequate to do so and that form factor dominance by vector mesons led to trouble at high q^2. There has been little change in the situation they described, e.g., the best subsequent models still not being formulated such that an isospin reflection connects realistic descriptions of the proton and neutron [4]. Because of this awkward situation regarding suitable dynamical models for the form

factors, it is desirable to ask the data to provide as many answers as possible to questions which can be formulated without a committment to the restrictive details of particular models.

Schumacher examines the symmetry content of (1) and its dynamical implications, and finds that the form of the deviations from (1) suggests a particular type of symmetry breaking, well known in the physics of strong interactions. From these considerations a broken symmetry theory of the form factors is formulated. Using the world's e-p data, Schumacher obtains several measures of symmetry breaking, which imply an oscillating G_{En} whose sign and magnitude agree with the Krohn-Ringo slope [14]. He further derives a set of scaling laws which relates the form factors G_{Mp} and G_{Mn} to G_{Ep} and G_{En}. These relations are

$$\begin{aligned} G_{Mp} &= \mu_p G_{Ep} + \mu_n G_{En} \\ G_{Mn} &= \mu_n G_{Ep} + \mu_p G_{En} \end{aligned} \qquad (4)$$

where $G_{Ep} = G_{ES} + G_{EV}$ is the "symmetry-conserving" part and $G_{En} = G_{ES} = G_{EV}$ is the "symmetry-violating" part of the form factors. These conclusions are primarily model-independent and do not require pole dominance of the spectral functions.

It is then, the purpose of this thesis to:

(a) Test the two forms of the scaling laws using the data of Bumiller and others [19] in the range $0.10 \le q^2 \le 0.80\ F^{-2}$, and

(b) To introduce a method of finding the ratio G_{En}/G_{Ep} without using the scaling laws, thus finding information about G_{En}.

II. THEORY

A. GENERAL

Jankus [7], found that for the deuteron

$$\frac{d\sigma}{d\Omega} = \left(\frac{d\sigma}{d\Omega}\right)_{Mott} \left(1 + \frac{2E}{M_D C^2} \sin^2 \frac{\Theta}{2}\right)^{-1} \left[D_C^2(q^2) + \frac{8}{9} \eta^2 D_Q^2(q^2) \right.$$

$$\left. + \frac{2}{3} \eta (1 + 2(1+\eta) \tan^2 \frac{\Theta}{2})\ D_M^2(q^2) \right] \tag{5}$$

where

$$D_C(q^2) = \int_0^\infty \left[u^2(r) + w^2(r) \right] j_0(\tau) dr \tag{6}$$

is the charge structure factor,

$$D_Q(q^2) = \frac{6\sqrt{2}}{q^2} M_D^2 \int_0^\infty \left[u(r)w(r) - \frac{w^2(r)}{\sqrt{8}} \right] j_2(\tau) dr \tag{7}$$

is the quadrupole moment structure factor, and

$$D_M^M(q^2) = \int_0^\infty \left[u^2(r) - \tfrac{1}{2} w^2(r) \right] j_0(\tau) dr + \frac{1}{\sqrt{2}} \int_0^\infty \left[u(r)w(r) + \frac{w^2(r)}{\sqrt{8}} \right] j_2(\tau) dr \tag{8}$$

accounts for the contribution of the intrinsic magnetic moments of the proton and the neutron to the scattering process, and

$$D_M^E(q^2) = \frac{3}{2} \int_0^\infty w^2(r) \left[j_0(\tau) + j_2(\tau) \right] dr \tag{9}$$

is the magnetic contribution to the scattering process arising from the convection of charge in the deutron. Together (8) and

(9) are

$$D_M(q^2) = \tfrac{1}{2}\left[(\mu_p + \mu_n)2D_M^M + D_M^E\right] .$$

The static limits ($q^2 \to 0$) are

$$\begin{aligned} D_C(q^2) &\to 1 \\ D_Q(q^2) &\to M_D^2 Q \\ D_M^M(q^2) &\to 1 - \frac{3}{2} P_D \\ D_M^E(q^2) &\to \frac{3}{2} P_D . \end{aligned} \tag{10}$$

The j_o and j_2 are spherical Bessel functions, $\tau = |\vec{q}\,|r/2$, Q is the quadrupole moment, P_D the percentage D state, and the u(r) and w(r) are suitably chosen wave functions of the deuteron.

Adler [15], shows that in the impulse approximation, the charge, quadrupole, and magnetic form factors are given by (along with their static limits):

$$G_C \equiv (G_{Ep} + G_{En})\ D_C \xrightarrow[q^2 \to 0]{} 1 \tag{11}$$

and

$$G_Q \equiv (G_{Ep} + G_{En})\ D_Q \longrightarrow M_D^2 Q \tag{12}$$

and

$$G_M \equiv (G_{Ep} + G_{En})\ D_M^E + (G_{Mp} + G_{Mn})2D_M^M \longrightarrow \frac{M_D}{M_p}\,\mu_D \tag{13}$$

where the D's are given in equations (6) through (9). The step from a point deuteron to a finite size deuteron is thus carried out by the introduction of the free nucleon form factors. This step is justified by the impulse approximation.

Rewrite equation (5) as

$$\left(\frac{d\sigma}{d\Omega}\right)\bigg/\left(\frac{d\sigma}{d\Omega}\right)_{Mott} = G_D^2 = A(q^2) + B(q^2)\tan^2\frac{\theta}{2} \qquad (5a)$$

where

$$A(q^2) = G_C^2 + \frac{8}{9}\eta^2 G_Q^2 + \frac{2}{3}\eta\, G_M^2 \qquad (5b)$$

$$\eta = \frac{q^2}{4M_D^2 C^2}$$

and

$$B(q^2) = \frac{4}{3}\eta\, G_M^2 \qquad (5c)$$

where the approximation $1 + \eta \rightarrow 1$ has been used. Equation (13) can be simplified considerably by scaling, i.e.,

$$G_{MD} = \mu'_D G_{CD}, \quad \mu'_D = 1.71$$

and

$$\frac{G_{Mp}}{\mu p} = \frac{G_{Mn}}{\mu n} = G_{Ep}.$$

For the case of the deuteron

$$G_{MD} \equiv (G_{Ep} + G_{En})\mu'_D\, D_C. \qquad (14)$$

Then

$$G_D^2 = (G_{Ep} + G_{En})^2 [D_C^2(1 + \frac{2}{3}\eta\,\mu'^2_D + \frac{4}{3}\eta\,\mu'^2_D \tan^2\frac{\theta}{2}) + \frac{8}{9}\eta^2 D_Q^2]$$

or

$$G_D^2 = (G_{Ep} + G_{En})^2\, F'^2_D \qquad (15)$$

where F'^2_D is called the deuteron structure factor and is the same as the result of Jankus for point nucleons in the deuteron. From (15)

$$\frac{G_D}{G_{Ep}} = F'_D\left(1 + \frac{G_{En}}{G_{Ep}}\right). \qquad (16)$$

Again consider equation (5). If the quadrupole term is neglected (a contribution of order 10^{-4} or less) and $1 + \eta \simeq 1$

is used, (5) becomes

$$\left(\frac{d\sigma}{d\Omega}\right) / \left(\frac{d\sigma}{d\Omega}\right)_{Mott} = G_D^2 = G_E^2 + \frac{2}{3}\eta\,(1 + 2\tan^2\frac{\theta}{2})G_M^2$$

$$= (G_E^2 + \frac{2}{3}\eta\, G_M^2) + \frac{4}{3}\eta\, G_M^2 \tan^2\frac{\theta}{2}\ . \tag{17}$$

From this equation, using $\left(\frac{d\sigma}{d\Omega}\right) / \left(\frac{d\sigma}{d\Omega}\right)_{Mott}$ as the ordinate and $\tan^2 \theta/2$ as the abcissa, a linear plot can be made ("Rosenbluth plot"). Then G_{Md}^2 is given by the slope, and G_{Ed}^2 can be found from the intercept. This method, however, presumes that absolute measurements of the deuteron cross section are available. Since Stewarts measurements are relative, available data must be analyzed in an attempt to make the experimental cross sections absolute in a first order sense.

This task can be accomplished by considering the work of de Vries [16] and Buchanan [4]. De Vries collected all available proton data, and made a fit to these data using adjustable parameters so that a minimum was obtained in a χ^2 fit. Buchanan collected the world's proton, neutron, and deuteron data, and updated them. He checked the de Vries b' fit using the reanalyzed data, and concluded that this fit is the best to describe the proton form factors.

Stewart [10] measured

$$R = \left(\frac{d\sigma}{d\Omega}\right)_D^{exp} / \left(\frac{d\sigma}{d\Omega}\right)_p^{exp}\ . \tag{18}$$

If it is assumed that the de Vries b' fit gives G_p^2 absolutely, then

$$\left(\frac{d\sigma}{d\Omega}\right)_p^{abs} = (G_p^2)_{abs} \left(\frac{d\sigma}{d\Omega}\right)_p^{Mott}\ . \tag{19}$$

If the ratio

$$N = \left(\frac{d\sigma}{d\Omega}\right)_p^{abs} / \left(\frac{d\sigma}{d\Omega}\right)_p^{exp} \tag{20}$$

is formed, N can be considered to be the factor required to normalize the experimental data to absolute data in a first order sense. Then, since the ratio R was measured

$$\left(\frac{d\sigma}{d\Omega}\right)_D^{theor} = \left(\frac{d\sigma}{d\Omega}\right)_D^{exp} (N) \tag{21}$$

can be considered to be absolute in the first order. The subscript theoretical is used to distinguish absolute in the first order from absolute.

Thus Rosenbluth plots for the deuteron may be made, and G_{ED}^2 and G_{MD}^2 can be extracted. If the scaling law holds, then within experimental error

$$\frac{G_{MD}}{\mu_D' G_{ED}} = 1.$$

B. SCALING APPLIED TO MAGNETIC CORRECTIONS

To eliminate the magnetic contribution to G_D^2 and G_P^2, the magnetic contribution is given by equation (15) as

$$C_D = \frac{2}{3}\eta_D \mu_D'^2 (1 + 2 \tan^2 \frac{\theta}{2}) \tag{22}$$

so that

$$G_{ED}^2 = \frac{G_D^2 \text{ exp}}{(1+C_D)} \tag{23}$$

with

$$G_D^2\text{exp} = \left(\frac{d\sigma}{d\Omega}\right)_D^{exp} / \left(\frac{d\sigma}{d\Omega}\right)_D^{Mott}$$

where the quadrupole terms has been neglected.

For the proton, the magnetic contribution is found by considering

$$G_p^2 = \frac{G_{Ep}^2}{1+\eta_p} + \eta_p \frac{G_{Mp}^2}{1+\eta_p} (1 + 2 \tan^2 \frac{\theta}{2}). \qquad (24)$$

Scaling assumes $G_{Mp} = \mu_p G_{Ep}$, where $\mu_p = 2.973$, so,

$$G_p^2 = \frac{G_{Ep}^2}{1+\eta_p} (1 + \eta_p \mu_p^2 (1 + 2 \tan^2 \frac{\theta}{2})). \qquad (24a)$$

The term

$$C_p = \eta_p \mu_p^2 (1 + 2 \tan^2 \frac{\theta}{2}) \qquad (25)$$

is then the magnetic correction term for the proton. Thus

$$G_{Ep}^2 = \frac{G_p^2 (1 + \eta_p)}{1 + C_p} \qquad (26)$$

where

$$G_p^2 = \left(\frac{d\sigma}{d\Omega}\right)_p^{exp} \Big/ \left(\frac{d\sigma}{d\Omega}\right)_p^{Mott} .$$

From his experiment, Stewart [10] calculated

$$\frac{G_{En}}{G_{Ep}} = \frac{1}{F_D} \frac{G_{ED}}{G_{Ep}} - 1$$

and evaluates from his data

$$\frac{G_{ED}^2}{G_{Ep}^2} = \frac{E K_D}{F K_p} \qquad (27)$$

where the E and F contain radiative corrections, Mott cross sections, target parameters and experimental counting rates.

Of interest here is the ratio K_D/K_p, which represents the magnetic correction terms, it is given by

$$\frac{K_D}{K_p} = \frac{1 + C_p}{(1+C_D)(1+\eta_p)} \qquad (28)$$

where C_D and C_p were defined by (22) and (25). This ratio contains the scaling law assumptions.

Next consider the scaling law proposed by Schumacher [4]. Specifically

$$G_{Mp} = \mu_p G_{Ep} + \mu_n G_{En} \tag{29}$$

$$G_{Mn} = \mu_n G_{Ep} + \mu_p G_{En} .$$

For the deuteron, consider similiar scaling laws

$$G_{MD} = \mu'_D G_{ED} + \mu_n G_{En} \tag{30}$$

$$G_{Mn} = \mu_n G_{ED} + \mu'_D G_{En} .$$

Then equation (17) becomes, neglecting terms containing G_{En}^2,

$$G_{ED}^2 = (G_{Ep} + G_{En})^2 D_C^2 \left[1 + \frac{2}{3}\eta_D \mu_D'^2 (1 + 2\tan^2 \frac{\theta}{2}) \right. \tag{31}$$

$$\left. + \frac{G_{Ep} G_{En}}{G_{Ep} + G_{En}} \left(\frac{4}{3} \frac{\eta_D \mu_n \mu'_D}{D_C} (1 + 2\tan^2 \frac{\theta}{2}) \right) \right] . \tag{32}$$

Now define

$$C_D^S = \left(\frac{2}{3}\eta_D \mu'_D + \frac{4}{3} \frac{G_{Ep} G_{En}}{G_{Ep} + G_{En}} \frac{\eta_D \mu_n}{D_C} \mu'_D \right) \left(1 + 2\tan^2 \frac{\theta}{2} \right) . \tag{32}$$

Similarily, for the proton equation (24) becomes, with the use of equation (29),

$$G_p^2 = \frac{G_{Ep}^2}{1+\eta_p} \left[1 + \left(\eta_p \mu_p^2 + 2\eta_p \mu_p \mu_n \frac{G_{En}}{G_{Ep}} \right) \left(1 + 2\tan^2 \frac{\theta}{2} \right) \right] \tag{33}$$

and define

$$C_p^S = \left(\eta_p \mu_p^2 + 2\eta_p \mu_p \mu_n \frac{G_{En}}{G_{Ep}} \right) \left(1 + 2\tan^2 \frac{\theta}{2} \right) . \tag{34}$$

Thus when using Schumacher's scaling, the magnetic correction ratio becomes

$$\frac{K_D^S}{K_p^S} = \frac{(1 + C_p^S)}{(1+C_D^S)(1+\eta_p)} . \tag{35}$$

It should be pointed out that equations (32), (34), and thus (35) contain the form factors G_{En} and G_{Ep}, both of which are sought from experiment. To use the readily available values from the de Vries b' fit would be combining the dipole fit with the broken symmetry theories, however these are needed for comparison of the scaling laws. If the de Vries b' fit values of G_{Ep} and G_{En} are incorrect at low q^2, their influence on equation (35) is quite small, so they will be used here.

A comparison of equations (28) and (35) gives a measure of the effect of the two scaling laws on the data of Stewart. These results are shown in Table VI.

C. DERIVATION OF AN EQUATION FOR G_{En}/G_{Ep} WITHOUT SCALING

This section has a threefold objective:

(a) Derivation of an expression for G_{En}/G_{Ep} without the use of scaling laws,

(b) Testing and comparison of the values of G_{En}/G_{Ep} obtained from the equation derived in (a) above, for $0.1 \leq q^2 \leq 0.8\ F^{-2}$, using de Vries b' fit, or proton scaling wherever required.

(c) Testing the effect of Schumacher's scaling on G_{En}/G_{Ep}.

To derive an expression for G_{En}/G_{Ep} without the use of scaling laws, use is made of equations previously introduced, specifically

$$G_C \equiv (G_{Ep} + G_{En})\, D_C \qquad (11)$$

and

$$G_M \equiv (G_{Ep} + G_{En})\, D_M^E + (G_{Mp} + G_{Mn}) 2\, D_M^M \qquad (13)$$

where D_C, D_M^M, and D_M^E are defined in equations (6), (8), and (9) respectively, and

$$G_D^2 = A(q^2) + B(q^2) \tan^2 \frac{\theta}{2}$$

$$A(q^2) = G_{CD}^2 + \frac{2}{3}\eta_D G_{MD}^2$$

$$B(q^2) = \frac{4}{3}\eta_D G_{MD}^2 . \tag{5a}$$

By the above equations,

$$G_D^2 = (G_{Ep} + G_{En})^2 D_C^2 + \frac{2}{3}\eta \left[(G_{Ep} + G_{En}) D_M^E + (G_{Mp} + G_{Mn}) 2D_M^M\right]^2 f(\theta) \tag{36}$$

where

$$f(\theta) \equiv 1 + 2 \tan^2 \frac{\theta}{2} .$$

For the proton, use equation (26)

$$G_p^2 = \frac{G_{Ep}^2}{1+\eta_p} + \left[\frac{\eta_p}{1+\eta_p} f(\theta) G_{Mp}^2\right]$$

and recall from equation (18)

$$R = \left(\frac{d\sigma}{d\Omega}\right)_D^{exp} \Big/ \left(\frac{d\sigma}{d\Omega}\right)_p^{exp} .$$

By taking the ratio G_d^2/G_p^2 it is possible to rearrange terms to find

$$\frac{G_D^2}{G_p^2} = R \frac{\left(\frac{d\sigma}{d\Omega}\right)_p^{Mott}}{\left(\frac{d\sigma}{d\Omega}\right)_D^{Mott}} = \frac{(G_{Ep}+G_{En})^2 D_C^2 + \frac{2}{3}\eta \left[(G_{Ep}+G_{En}) D_M^E + 2(G_{Mp}+G_{Mn}) D_M^M\right]^2 f(\theta)}{\frac{G_{Ep}^2}{1+\eta_p} + \frac{\eta_p}{1+\eta_p} f(\theta) G_{Mp}^2}$$

Again rearranging terms, end up with,

$$R \frac{\left(\frac{d\sigma}{d\Omega}\right)_p^{Mott}}{\left(\frac{d\sigma}{d\Omega}\right)_D^{Mott}} \left[\frac{F(\theta)}{1+\eta_p} + \frac{\eta_p}{1+\eta_p}\left(\frac{G_{Mp}^2}{G_{Ep}^2}\right)\right] = D_C^2 \left(\frac{G_{En}}{G_{Ep}} + 1\right)^2 F(\theta) \tag{37}$$

$$+ \frac{2}{3}\eta_D \left\{ D_M^{E^2} \left(\frac{G_{En}}{G_{Ep}}\right)^2 + 2D_M^{E^2}\left(\frac{G_{En}}{G_{Ep}}\right) + 4D_M^E D_M^M \left(\frac{G_{En}}{G_{Ep}}\right)\left(\frac{G_{Mp}+G_{Mn}}{G_{Ep}}\right)\right.$$

$$+ D_M^{E^2} + 4D_M^E D_M^M \left(\frac{G_{Mp}+G_{Mn}}{G_{Ep}}\right) + 4(D_M^M)^2 \left(\frac{G_{Mp}+G_{Mn}}{G_{Ep}}\right)^2 \Bigg\}$$

where

$$F(\theta) = f(\theta)^{-1} .$$

This equation is free of approximations and does not contain scaling.

To put equation (37) in to a form free of magnetic contributions, a resort to graphical methods at constant q^2 was made. The equation can be written in the form

$$Y = mX + b$$

where

$$Y = R \frac{\left(\frac{d\sigma}{d\Omega}\right)_p^{Mott}}{\left(\frac{d\sigma}{d\Omega}\right)_D^{Mott}} \left[\frac{F(\theta)}{1+\eta_p} + \frac{\eta_p}{1+\eta_p} \frac{G_{Mp}^2}{G_{Ep}^2}\right]$$

$$m = D_C^2 \left(\frac{G_{En}}{G_{Ep}} + 1\right)^2$$

$$X = F(\theta) = (1 + 2\tan^2\frac{\theta}{2})^{-1}$$

$$b = \frac{2}{3}\eta_D \Bigg\{ D_M^{E^2} \left(\frac{G_{En}}{G_{Ep}}\right)^2 + 2D_M^{E^2} \frac{G_{En}}{G_{Ep}} + 4D_M^E D_M^M \left(\frac{G_{En}}{G_{Ep}}\right)\left(\frac{G_{Mp}+G_{Mn}}{G_{Ep}}\right)$$

$$+ D_M^{E^2} + 4D_M^E D_M^M \left(\frac{G_{Mp}+G_{Mn}}{G_{Ep}}\right) + 4D_M^{M^2}\left(\frac{G_{Mp}+G_{Mn}}{G_{Ep}}\right)^2 \Bigg\} .$$

For constant q^2, X and Y are the only variable terms, $Y = f(R,\theta)$ and $X = f(\theta)$. The assumption was made that the error in G_{Mp}^2/G_{Ep}^2 for $0.1 \le q^2 \le 0.8\ F^{-2}$ has a negligible effect when compared to the error in R. It should be noted here that G_{Mp}^2/G_{Ep}^2 has to be obtained either from the scaling laws of the proton, or from the de Vries b' fit; a later discussion shows that it makes little difference which.

Using a least squares fit to the data for the above equations, the graphical methods were found to be relatively inaccurate.

The remedy to the above difficulty was to turn to an analytical method where the points were averaged using a weighted average method. Equation (37) can be rearranged to give

$$\frac{R\left(\frac{d\sigma}{d\Omega}\right)_p^{Mott}}{\left(\frac{d\sigma}{d\Omega}\right)_D^{Mott}}\left[\frac{F(\theta)}{1+\eta_p}+\frac{\eta_p}{1+\eta_p}\frac{G_{Mp}^2}{G_{Ep}^2}\right]=\left(\frac{G_{En}}{G_{Ep}}\right)^2\left(D_C^2\,F(\theta)+\frac{2}{3}\,\eta_D D_M^{E^2}\right)$$

$$+\left(\frac{G_{En}}{G_{Ep}}\right)\left(2D_C^2\,F(\theta)+\frac{4}{3}\eta_D\,D_M^{E^2}+\frac{8}{3}\,\eta_D\,D_M^E\,D_M^M\,S\right) \qquad (38)$$

$$+\left(D_C^2\,F(\theta)+\frac{2}{3}\,\eta_D\,D_M^{E^2}+\frac{8}{3}\,\eta_D\,D_M^E\,D_M^M\,S+\frac{8}{3}\,\eta_D\,D_M^{M^2}S^2\right)$$

where

$$S=\frac{G_{Mp}+G_{Mn}}{G_{Ep}} .$$

The assumption was made that every quantity can be taken to be exact (although the D's are based on theoretical models), except R, G_{Mp}^2/G_{Ep}^2, S, and consequently the unknown, G_{En}^2/G_{Ep}^2 .

Up to this point equation (38) is exact and contains no scaling, however, G_{Mp}^2/G_{Ep}^2, and S are as yet undetermined. There are two methods available to get G_{Mp}^2/G_{Ep}^2 since absolute data are not available. The methods are from the de Vries b' fit and the scaling laws.

If the de Vries b' fit is used,

$$\left(\frac{G_{Mp}}{G_{Ep}}\right)^2=\left(\frac{G_{Mp}}{G_{Ep}}\right)^2_{\text{de Vries}} .$$

$$S=\left(\frac{G_{Mp}+G_{Mn}}{G_{Ep}}\right)_{\text{de Vries}} .$$

If scaling is used,

$$\frac{G_{Mp}^2}{G_{Ep}^2} = \mu_p^2$$

$$S = \mu_p + \mu_n .$$

Now equation (38) is put into a more workable quadratic form

$$aX^2 + bX + c = 0$$

where $X = G_{En}/G_{Ep}$. By inspection

$$a = D_C^2 \, F(\theta) + \frac{2}{3} \eta_D \, D_M^{E^2}$$

$$b = 2D_C^2 \, F(\theta) + \frac{4}{3} \eta_D \, D_M^{E^2} + \frac{8}{3} \eta_D \, D_M^E \, D_M^M \, S$$

$$c = D_C^2 \, F(\theta) + \frac{2}{3} \eta_D \, D_M^{E^2} + \frac{8}{3} \eta_D \, D_M^E \, D_M^M \, S + \frac{8}{3} \eta_D \, D_M^{M^2} \, S^2$$

$$-R \frac{\left(\frac{d\sigma}{d\Omega}\right)_p^{Mott}}{\left(\frac{d\sigma}{d\Omega}\right)_D^{Mott}} \left[\frac{1}{1+\eta_p} F(\theta) + \frac{\eta_p}{1+\eta_p} \left(\frac{G_{Mp}}{G_{Ep}}\right)^2 \right]$$

The results of these two methods are summarized in Table VII.

By applying Schumacher's scaling to equation (38), a comparison of G_{En}/G_{Ep} can be made to that of the two methods discussed above.

In equation (38), the terms involving G_{Mp}^2/G_{Ep}^2, $S = \frac{G_{Mp}+G_{Mn}}{G_{Ep}}$, and S^2 are the only ones affected. Let $X = G_{En}/G_{Ep}$. Then by application of equation (4), it is seen that

$$\left(\frac{G_{Mp}}{G_{Ep}}\right)^2 = (\mu_p + \mu_n X)^2 \qquad (39)$$

and

$$S = (\mu_p + \mu_n)(1 + X) .$$

By rearranging terms after substituting equation (39) into equation (38), the resulting equation is

$$a'X^2 + b'X + c' = 0 \tag{40}$$

where

$$a' = D_C^2\, F(\theta) + \frac{2}{3}\,\eta_D\, D_M^{E^2} - R\,\frac{\left(\frac{d\sigma}{d\Omega}\right)_p^{Mott}}{\left(\frac{d\sigma}{d\Omega}\right)_D^{Mott}}\;\frac{\eta_p}{1+\eta_p}\,\mu_n^2 + \frac{8}{3}\,\eta_D D_M^E D_M^M\,(\mu_p+\mu_n) + \frac{8}{3}\,\eta_D D_M^{M^2}\,(\mu_p+\mu_n)^2 \tag{40a}$$

$$b' = 2D_C^2\, F(\theta) + \frac{4}{3}\,\eta_D\, D_M^{E^2} + 2\left[\frac{8}{3}\,\eta_D\, D_M^E\, D_M^M\,(\mu_p+\mu_n)\right]$$

$$+\;2\left[\frac{8}{3}\,\eta_D\, D_M^{M^2}\,(\mu_p+\mu_n)^2\right] - R\,\frac{\left(\frac{d\sigma}{d\Omega}\right)_p^{Mott}}{\left(\frac{d\sigma}{d\Omega}\right)_D^{Mott}}\;\frac{\eta_p}{1+\eta_p}\,\mu_p\mu_n \tag{40b}$$

and

$$c' = c = D_C^2\, F(\theta) + \frac{2}{3}\,\eta_D\, D_M^{E^2} + \frac{8}{3}\,\eta_D\, D_M^E\, D_M^M\,(\mu_p+\mu_n)$$

$$+\;\frac{8}{3}\,\eta_D\, D_M^{M^2}\,(\mu_p+\mu_n)^2$$

$$-R\,\frac{\left(\frac{d\sigma}{d\Omega}\right)_p^{Mott}}{\left(\frac{d\sigma}{d\Omega}\right)_D^{Mott}}\;\left[\frac{F(\theta)}{1+\eta_p} + \frac{\eta_p}{1+\eta_p}\,\mu_p^2\right]. \tag{40c}$$

III. REEVALUATION OF EXPERIMENTAL DATA

A. DATA

The data analyzed here were collected by Bumiller and others [19] at the Naval Postgraduate School linear accelerator in the range $0.1 \le q^2 \le 0.4\ F^{-2}$, and at the Mark III accelerator at Stanford University in the range $0.2 \le q^2 \le 0.8\ F^{-2}$. The experimental set up was basically the same in both laboratories. Whenever possible, overlapping sets of data were taken to check for any systematic errors in the equipment. No systematic deviations between the two sets of measurements were found and the data analysis was performed independent of the source. Table I shows the data used in these analyses, with the error listed.

B. ROSENBLUTH PLOTS

Equation (17) formed the basis for the Rosenbluth plots. This equation was broken up as follows for the plots:

$$Y = \left(\frac{d\sigma}{d\Omega}\right)_D^{\text{theor}} \Big/ \left(\frac{d\sigma}{d\Omega}\right)_D^{\text{Mott}} \tag{17a}$$

$$X = \tan^2 \frac{\theta}{2}$$

where

$$\left(\frac{d\sigma}{d\Omega}\right)_D^{\text{theor}} = R(G_p^2)_{abs} \left(\frac{d\sigma}{d\sigma}\right)_p^{\text{Mott}}$$

and R is given by equation (18). Wherever appropriate, weighted averages were used, and the corresponding error calculated. A weighted least squares fit was used to determine the slope and intercept, with the error in each. This method is described in Appendix C.

Since these plots were made for a constant q^2, it is readily apparent that from the slope m,

$$G_{MD}^2 (q^2) = \frac{3}{4} \frac{m}{\eta_D}$$

and from the slope m and intercept b,

$$G_{ED}^2 (q^2) = b - \tfrac{1}{2}m.$$

Table III gives the results of these plots for the deuteron, and a sample plot is shown in Figure 1.

C. MAGNETIC CORRECTIONS

The magnetic correction gives the number by which the experimental G_p^2 or G_d^2 is to be multiplied to remove the magnetic contributions and yield G_{Ep}^2 or G_{Ed}^2. These corrections were computed using equations (22), (25), (27), (32), (34), and (35). The D_c term contained in equation (32) is the charge structure factor and is given by equation (6), with the Feshbach-Lomom wave functions [11] being used to describe the deuteron. Values of D_c are listed in Table III. The magnetic corrections using both scaling laws, a comparison of the resulting corrections, and the effect of magnetic corrections using Schumacher scaling on G_{En}/G_{Ep} as calculated by Stewart are shown in Table VI. The error was calculated by taking K_D/K_p as the standard value.

D. CALCULATION OF G_{En}/G_{Ep} WITHOUT SCALING

Equation (38) is the basis for these calculations. The D_c, D_M^E, and D_M^M are respectively, the charge structure factor, magnetic contribution to the scattering process arising from the convection of charge in the deuteron, and the contribution of the intrinsic

magnetic moments of the proton and the neutron to the scattering process. These factors are given by equations (5), (8), and (9). As with the magnetic corrections, the Feshbach-Lomom wave functions were used. The values of these wave functions at the appropriate q^2 are also listed in Table III.

G_{Mp}^2/G_{Ep}^2 is contained within equation (38) and is an undetermined quantity. Since absolute data are not available, this ratio may be found from the de Vries b' fit, or from the proton scaling law. Both methods of calculation were used, and it was found that they differ by a small percentage.

Results of these calculations are listed in Table VII, and a comparison of G_{En}/G_{Ep} computer using data from de Vries b' fit, and using proton scaling is shown in Figure 5.

E. CALCULATION OF G_{En}/G_{Ep} USING SCHUMACHER SCALING

These calculations were made using equation (40), with the coefficients given by equations (40a-c). As in the previous calculations the D_c, D_M^E, and D_M^M were calculated using the Feshbach-Lomom wave functions as listed in Table III.

IV. PRESENTATION OF RESULTS, DISCUSSION, AND CONCLUSIONS

A. PRESENTATION OF RESULTS, AND DISCUSSION

The experimental data are presented in Table I. The errors quoted are attributed to counting and target thickness errors, and are the only errors that enter into a ratio experiment.

Table II shows the Mott cross sections for point proton and deuteron in the laboratory system; $G_p^2(q^2)$ from the b' fit of de Vries is the absolute form factor for the proton; the theoretical cross sections as described in Section IIA; and the normalization factor N required to make the experimental deuteron cross section absolute in the first order sense.

Shown in Table III are the quantities D_c, D_M^E, D_M^M as described in Sections IIA, computed from the Feshbach-Lomom wave functions without relativistic corrections.

Table IV lists the magnetic and electric form factors of the deuteron as calculated from the Rosenbluth plots. Figures 2 and 3 illustrate these results. It is seen from Figure 2 that the electric form factors approach the static limit as predicted by the theory. From Figure 3 it is seen that the magnetic form factors are to large by a factor of three. This is due in part to the fact that G_{MD} is a function of the slope of the linear plot and is very senstive to experimental errors. A weighted least squares plot was used in an attempt to minimize the error. Also shown in Table IV is the ratio $\frac{G_{MD}}{\mu'_D G_{ED}}$. If scaling is to hold, this ratio must be unity, within experimental error. It is seen

however, that within experimental error $\frac{G_{MD}}{\mu'_D G_{ED}} \approx 3$, indicating that scaling does not hold. Since the values of G_{MD} are about three times larger than predicted, it must be held that this test is inconclusive.

To investigate the effect of magnetic contributions to the electric form factor, and get information as to the importance of scaling within the range of q^2 of interest, the Rosenbluth plots were considered. From these plots it was seen that

$$G_{ED}^2 = f(b,m)$$

where b is the Y intercept, and m is the slope of the linear plot. Specifically,

$$G_{ED}^2 = b - \tfrac{1}{2} m$$

where m contains the magnetic contribution. Define

$$G_{ED}^{*2} = b$$

where G_{ED}^* is the electric form factor without magnetic contributions. Table V shows the results of these calculations. The result is that a very small error is introduced if the magnetic contributions are disregarded, thus concluding that scaling has little effect in the range of q^2 considered here.

Stewart [10] was interested in the ratio G_{ED}/G_{Ep}, from which he finds G_{En}/G_{Ep}. It was shown in Section IIB, that the ratio G_{ED}/G_{Ep} contains the magnetic correction ratio, which in turn contains the scaling laws. Using both scaling laws, a comparison was made of the two magnetic correction ratios. Table IV contains these results, showing that the difference in the corrections is small, but tend to increase with q^2.

Table VII shows four sets of values of G_{En}/G_{Ep} as obtained:

(a) Without using scaling, but using the assumption of the de Vries

b' fit; (b) By using proton scaling in the form $G_{Mp} = \mu_p G_{Ep}$; (c) By Using Schumacher's scaling law for the proton and; (d) As calculated by Stewart [10]. In each case the Feshbach-Lomom wave functions were used, and relativistic corrections described by Stewart were applied. Each of the columns shows the slopes $d(G_{En}/G_{Ep})/dq^2$, calculated by using a weighted least squares fit. In each case the slopes are in good agreement.

B. CONCLUSIONS

Based upon the experimental data available in the range of momentum transfers of interest here, the following conclusions can be made:

(a) Both forms of scaling as applied to the deuteron form factor have negigible effect on the ratio G_{En}/G_{Ep}.

(b) The application of either scaling law to the proton form factor results in nearly identical corrections to the ratio G_{En}/G_{Ep}, thus allowing no distinction between them.

(c) The agreement of the experimental data with the neutron-electron interaction slope at $q^2 \approx 0$ is not influenced by the choice of the scaling law.

Although both forms of scaling give satisfactory results in the momentum transfer range investigated here, the Schumacher scaling appears to be on a better theoretical basis, and should be tested at higher momentum transfers. A conclusive test for the scaling laws would require an improvement in experimental accuracy by at least an order of magnitude, a technically nearly impossible requirement.

The interpretation of measurements at higher momentum transfers, where the difference between the scaling laws would be more pronounced is hampered by increased difficulties in the theoretical prediction of deuteron wave functions.

In agreement with Stewart, an important qualitative conclusion from these analyses is that the neutron has a non-zero charge form factor, not affected by the choice of scaling laws, implying a charge distribution within the neutron. The neutron will then have a charge structure with the outermost part of the charge distribution being negative in sign.

APPENDIX A. TABLES

TABLE I. EXPERIMENTAL DATA

q^2 F^{-2}	θ	$\left(\frac{d\sigma}{d\Omega}\right)_D$ $\times 10^{-30}$ cm^2 Monterey	$\left(\frac{d\sigma}{d\Omega}\right)_p$ $\times 10^{-30}$ cm^2 Monterey	R	% Error in R	$\left(\frac{d\sigma}{d\Omega}\right)_D$ $\times 10^{-30}$ cm^2 Stanford	$\left(\frac{d\sigma}{d\Omega}\right)_p$ $\times 10^{-30}$ cm^2 Stanford
0.1	45^o	20.54	23.88	0.8601	1.82		
	75^o	7.202	7.788	0.9247	2.28		
	90^o	3.577	3.892	0.9191	1.72		
0.2	45^o			0.7721	1.62	9.79	12.68
	45^o			0.7618	1.62	9.66	12.68
	45^o			0.8682	2.12	10.41	11.99
	45^o			0.8432	2.12	10.11	11.99
	75^o	2.796	3.574	0.7823	1.42		
	120^o	0.560	0.681	0.8223	1.18		
0.3	45^o			0.7025	1.60	5.165	7.352
	75^o	1.611	2.276	0.7078	2.00		
	90^o	0.911	1.259	0.7236	1.22		
	105^o	0.541	0.766	0.7063	1.28		
0.4	45^o			0.6414	1.80	3.873	6.038
	45^o			0.6601	1.50	3.986	6.038
	45^o			0.6812	1.76	3.647	5.354
	90^o	0.594	0.925	0.6422	1.24		
0.5	60^o			0.5876	1.60	2.044	1.201
0.6	60^o			0.5322	1.42	1.726	0.919
0.8	75^o			0.4565	1.80	0.668	0.305

TABLE II *

MOTT CROSS SECTIONS, $G_p^2(b')$, $\left(\frac{d\sigma_p}{d\Omega}\right)_{theor}$, N, $\left(\frac{d\sigma_D}{d\Omega}\right)_{theor}$

q^2 F^{-2}	θ	$\left(\frac{d\sigma_p}{d\Omega}\right)_{Mott}$ $\times 10^{-30}$ cm^2	$\left(\frac{d\sigma_D}{d\Omega}\right)_{Mott}$ $\times 10^{-30}$ cm^2	$G_p^2(b')$	$\left(\frac{d\sigma_p}{d\Omega}\right)_{theor}$	N	$\left(\frac{d\sigma_D}{d\Omega}\right)_{theor}$
0.1	45°	29.50	30.27	0.9866	29.10	1.219	25.01
	75°	8.344	8.687	0.9937	8.291	1.065	7.662
	90°	4.848	5.082	1.0000	4.848	1.246	4.459
0.2	45°	14.45	14.97	0.9735	14.07	1.134	11.25
	75°	4.034	4.271	0.9872	3.982	1.114	3.114
	120°	0.7544	0.8184	1.066	0.8042	1.133	0.6618
0.3	45°	9.475	9.901	0.9606	9.102	1.238	6.394
	75°	2.621	2.811	0.9806	2.570	1.129	1.818
	90°	1.509	1.637	1.0000	1.509	1.199	1.092
	105°	0.8709	0.9542	1.034	0.9005	1.176	0.6360
0.4	45°	7.011	7.376	0.9479	6.646	1.144	4.392
	90°	1.104	1.212	0.9996	1.104	1.194	0.7083

* Weighted averages are used wherever applicable

TABLE III

D_C, D_M^M AND D_M^E COMPUTED FROM

FESHBACH-LOMOM WAVE FUNCTIONS

q^2 F^{-2}	D_C	D_M^M	D_M^E
0.1	0.9397	0.8702	0.0729
0.2	0.8866	0.8214	0.0717
0.3	0.8396	0.7783	0.0705
0.4	0.7974	0.7398	0.0693
0.5	0.7592	0.7051	0.0682
0.6	0.7245	0.6736	0.0672
0.8	0.6636	0.6186	0.0651

TABLE IV

DEUTERON MAGNETIC AND ELECTRIC FORM FACTORS FROM ROSENBLUTH PLOTS

q^2 F^{-2}	Θ	X	Y	Slope	Intercept	G_{MD}	G_{ED}	$\frac{G_{MD}}{\mu'_D G_{ED}}$
0.1	45°	0.1716	0.8270±0.0151					
	75°	0.5888	0.8821±0.0201	0.0589±0.0450	0.8250±0.0318	11.77 ±5.42	.8919±0.0551	7.659±5.420
	90°	1.0000	0.8774±0.0151					
0.2	45°	0.1716	0.7516±0.0068					
	75°	0.5888	0.7294±0.0104	0.0220±0.0068	0.7397±0.0113	4.732±1.977	0.8536±0.0132	3.237±1.977
	120°	3.0000	0.8080±0.0095					
0.3	45°	0.1716	0.6458±0.0103					
	75°	0.5888	0.6471±0.0129	0.0148±0.0171	0.6451±0.0197	3.481±1.968	0.7986±0.0261	2.549±1.968
	90°	1.0000	0.6670±0.0081					
	105°	1.6984	0.6666±0.0085					
0.4	45°	0.1716	0.5956±0.0057					
	90°	1.0000	0.5847±0.0073	-0.01298±0.158	0.5980±0.0099	2.920±1.516	0.7775±0.0186	2.193±1.516

TABLE V

EFFECT OF G_{MD} ON G_{ED} BASED ON ROSENBLUTH PLOT

q^2 F^{-2}	G_{ED}	$\frac{2}{3}\eta\, G_{MD}^2$	G_{ED}^*	Error %
0.1	0.8919	0.0294	0.9083	1.84
0.2	0.8536	0.0110	0.8601	0.761
0.3	0.7986	0.0074	0.8032	0.576
0.4	0.7775	-0.0065	0.7733	0.540

TABLE VI

MAGNETIC CORRECTIONS* AND EFFECT ON $\frac{G_{ED}}{G_{EP}}$ COMPUTED BY STEWART

q^2 F^{-2}	θ	K_D	K_P	K_D/K_P	K_D^S	K_P^S	K_D^S/K_P^S	Error	% Change in Error in GED/GEP
0.1	45°	.9993	.9897	1.0097	.9990	.9897	1.0094	.0297	0.0000
	75°	.9988	.9828	1.0163	.9984	.9827	1.0159	.0403	0.0002
	90°	.9984	.9760	1.0230	.9977	.9760	1.0223	.0665	0.0006
0.2	45°	.9985	.9796	1.0193	.9978	.9760	1.0224	.300	0.0106
	75°	.9976	.9661	1.0326	.9964	.9662	1.0313	.127	.0028
	120°	.9925	.8948	1.1092	.9885	.8950	1.1055	.425	.0371
0.3	45°	.9978	.9697	1.0290	.9964	.9699	1.0272	.171	.0046
	75°	.9965	.9500	1.0489	.9941	.9503	1.0461	.268	.0090
	90°	.9951	.9313	1.0685	.9919	.9317	1.0646	.369	.0273
	105°	.9929	.9014	1.1015	.9881	.9018	1.0957	.530	.0527
0.4	45°	.9971	.9601	1.0385	.9948	.9605	1.0357	.272	.0109
	90°	.9935	.9106	1.0910	.9883	.9113	1.0845	.600	.0688
0.5	60°	.9955	.9383	1.0610	.9912	.9391	1.0555	.518	.0414
0.6	60°	.9946	.9270	1.0729	.9887	.9281	1.0654	.704	.0825
0.8	75°	.9906	.8772	1.1293	.9777	.8798	1.1113	1.60	.3017

* The magnetic correction gives the number by which the G_p^2 or G_d^2 is to be multiplied to remove the magnetic contributions and yield G_{Ep}^2 or G_{ED}^2.

TABLE VII

G_{En}/G_{Ep} COMPUTED WITHOUT SCALING, WITH PROTON SCALING, WITH SCHUMACHER SCALING, AND AS COMPUTED BY STEWART

q^2 (F^{-2})	ΔG_{En}	Without Scaling	Proton Scaling	Schumacher Scaling	Stewart
0.10	0.0006	-0.00315 $\pm$ 0.0058	-0.00314 $\pm$ 0.0058	-0.00315 $\pm$ 0.0058	-0.0020 $\pm$ 0.0055
0.20	0.0012	0.00373 $\pm$ 0.0033	0.00379 $\pm$ 0.0033	0.00341 $\pm$ 0.0033	0.0052 $\pm$ 0.0032
0.30	0.0018	0.00131 $\pm$ 0.0037	0.00178 $\pm$ 0.0037	0.00169 $\pm$ 0.0037	0.0012 $\pm$ 0.0038
0.40	0.0024	0.01079 $\pm$ 0.0039	0.01095 $\pm$ 0.0039	0.01065 $\pm$ 0.0039	0.0103 $\pm$ 0.0038
0.50	0.0030	0.00477 $\pm$ 0.0081	0.00499 $\pm$ 0.0081	0.00489 $\pm$ 0.0081	0.0069 $\pm$ 0.0079
0.60	0.0036	0.00474 $\pm$ 0.0072	0.00502 $\pm$ 0.0072	0.00494 $\pm$ 0.0072	0.0048 $\pm$ 0.0071
0.80	0.0048	0.01913 $\pm$ 0.0066	0.01977 $\pm$ 0.0066	0.01839 $\pm$ 0.0066	0.0197 $\pm$ 0.0055
	Slope	0.0245 $\pm$ 0.0098	0.0253 $\pm$ 0.0098	0.0243 $\pm$ 0.0098	0.0231 $\pm$ 0.0096
	Intercept	-0.0031 $\pm$ 0.0037	-0.0031 $\pm$ 0.0037	-0.0031 $\pm$ 0.0037	-0.0020 $\pm$ 0.0036

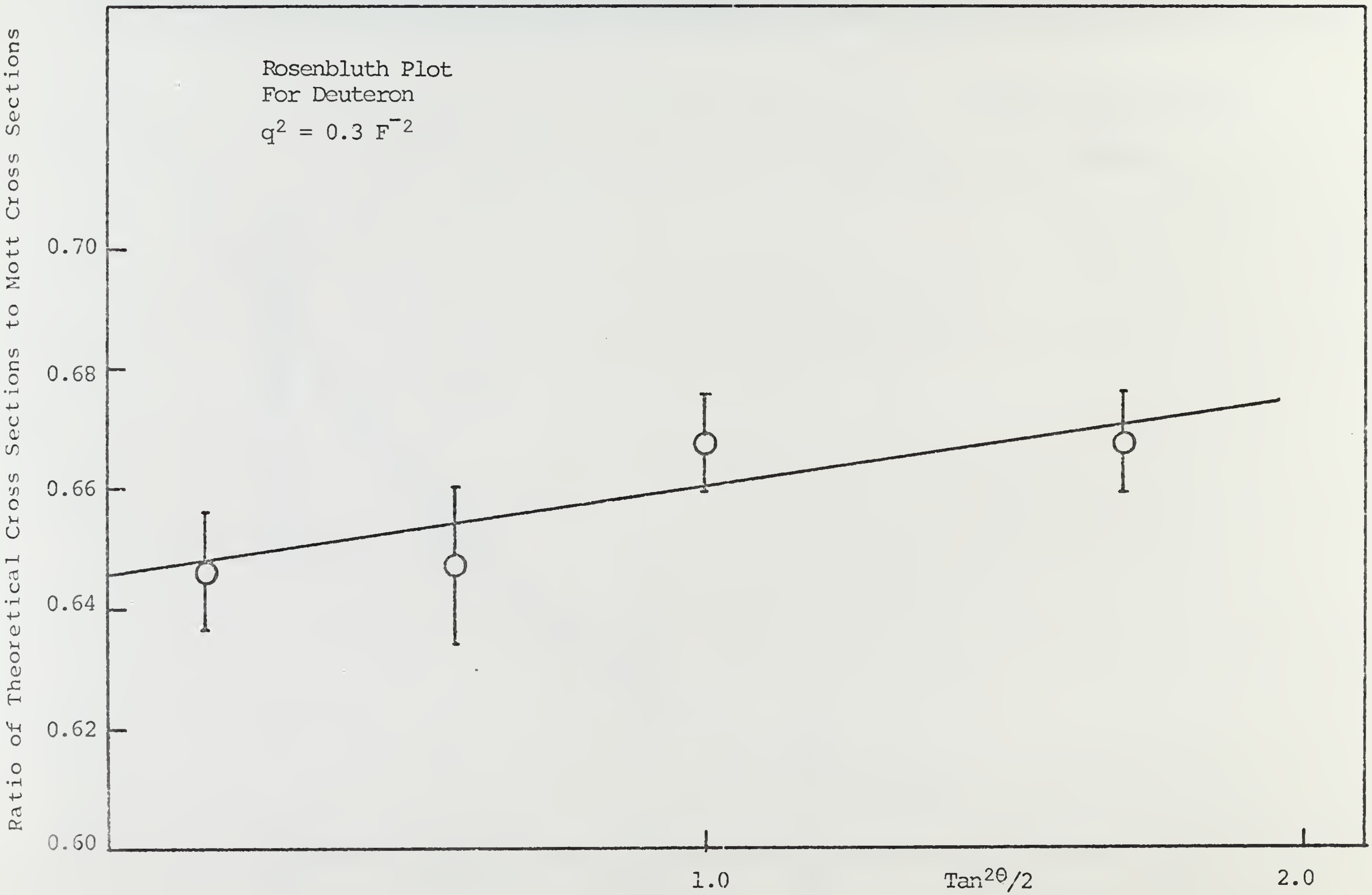
Rosenbluth Plot
For Deuteron
q2 = 0.3 F-2
Ratio of Theoretical Cross Sections to Mott Cross Sections
0.70
0.68
0.66
0.64
0.62
0.60
1.0
Tan2θ/2
2.0

Figure 1

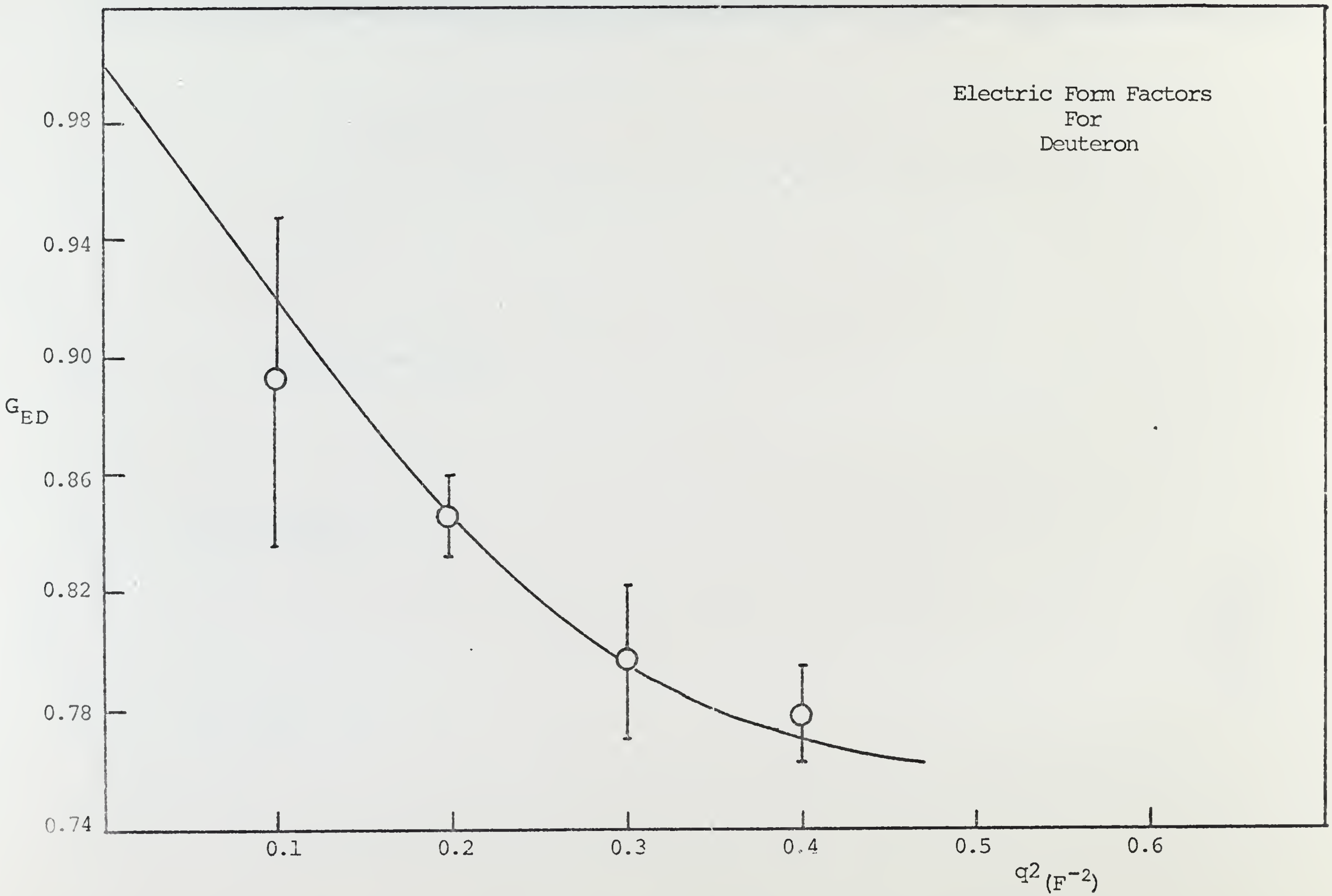
Electric Form Factors
For
Deuteron
G_{ED}
0.98
0.94
0.90
0.86
0.82
0.78
0.74
0.1
0.2
0.3
0.4
0.5
0.6
$q^2 (F^{-2})$

Figure 2

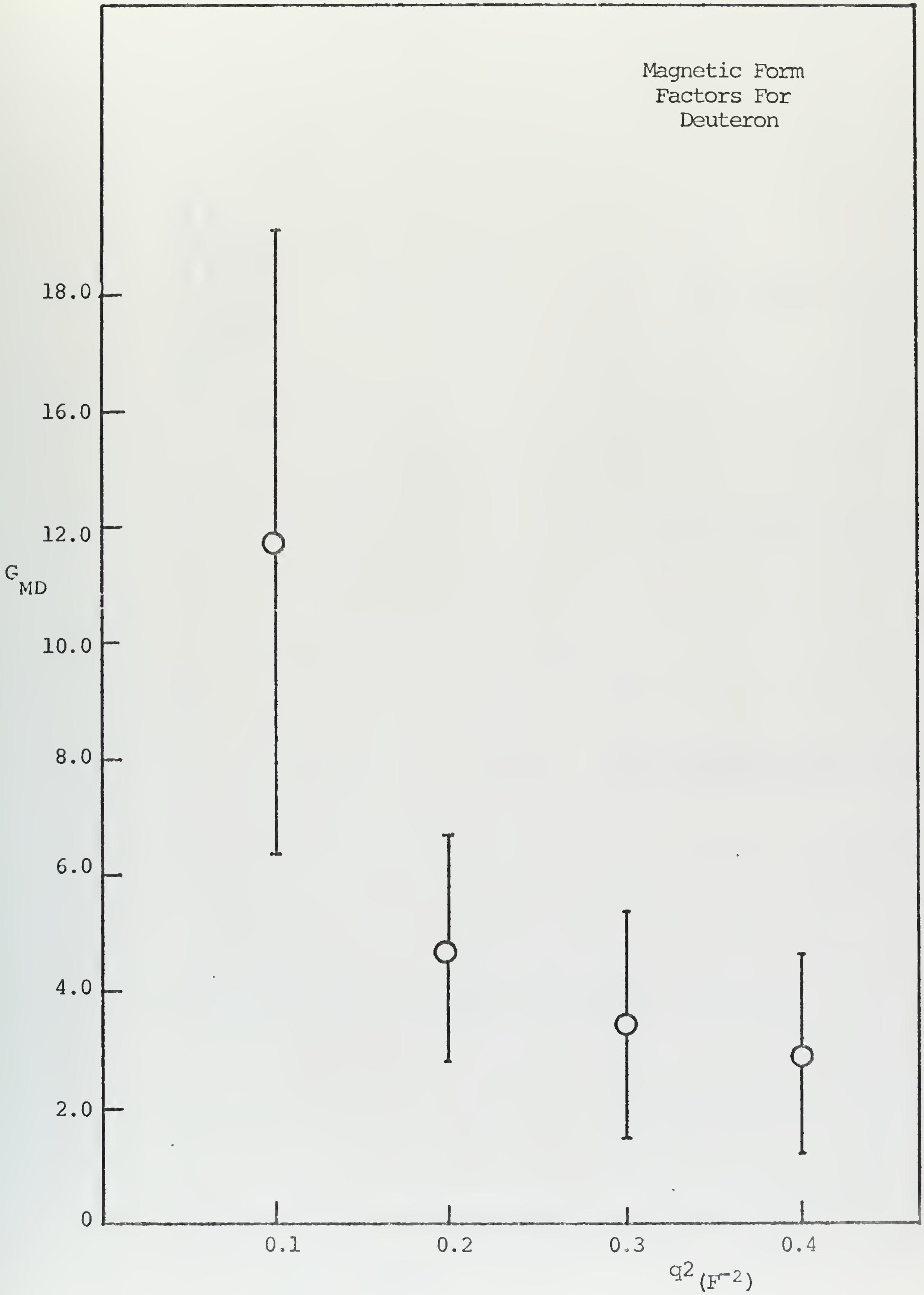

Magnetic Form
Factors For
Deuteron
18.0
16.0
12.0
G_{MD}
10.0
8.0
6.0
4.0
2.0
0
0.1
0.2
0.3
0.4
q^2 (F^{-2})

Figure 3

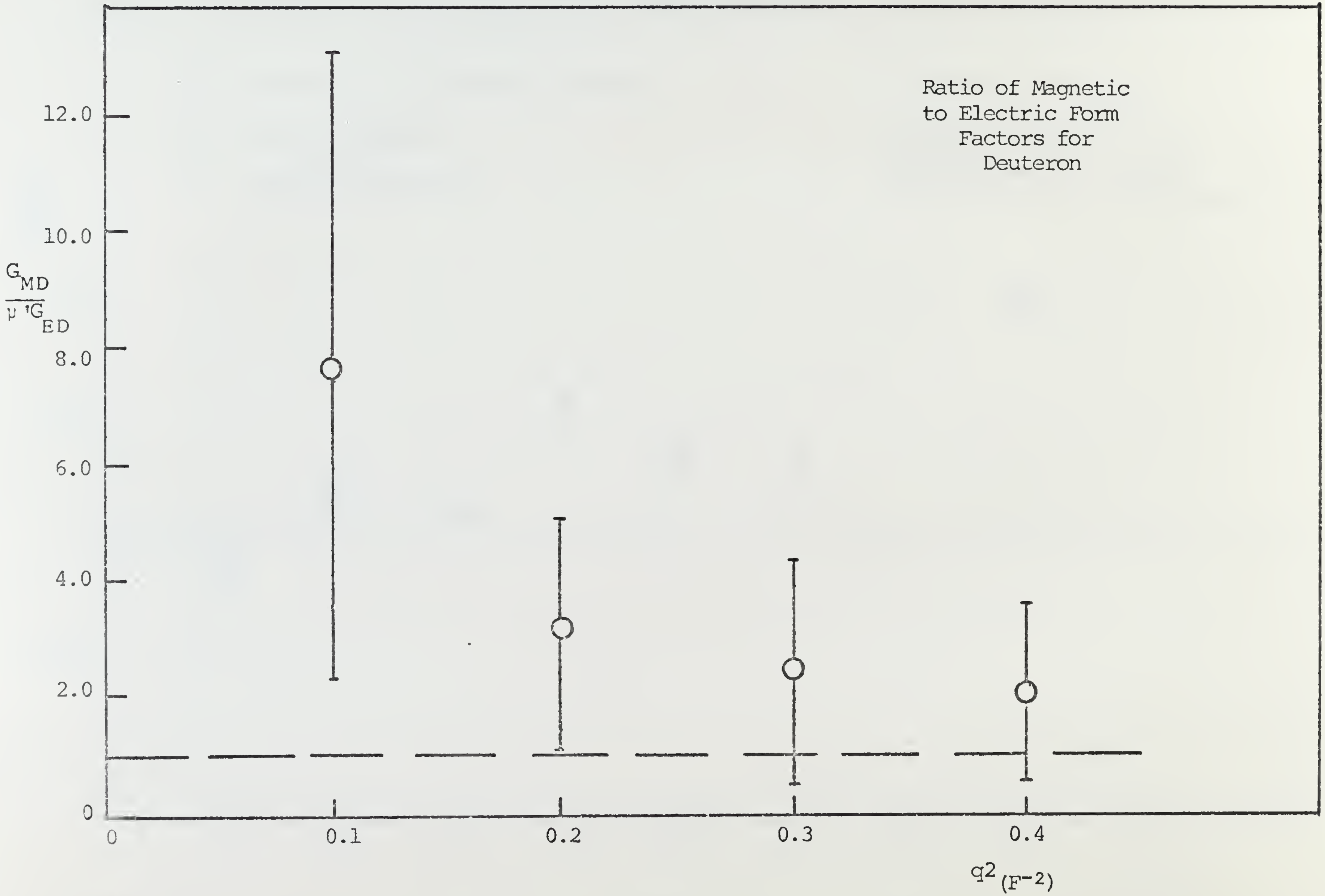

Ratio of Magnetic to Electric Form Factors for Deuteron
$\frac{G_{MD}}{\mu' G_{ED}}$
12.0
10.0
8.0
6.0
4.0
2.0
0
0
0.1
0.2
0.3
0.4
q^2 (F^{-2})

Figure 4

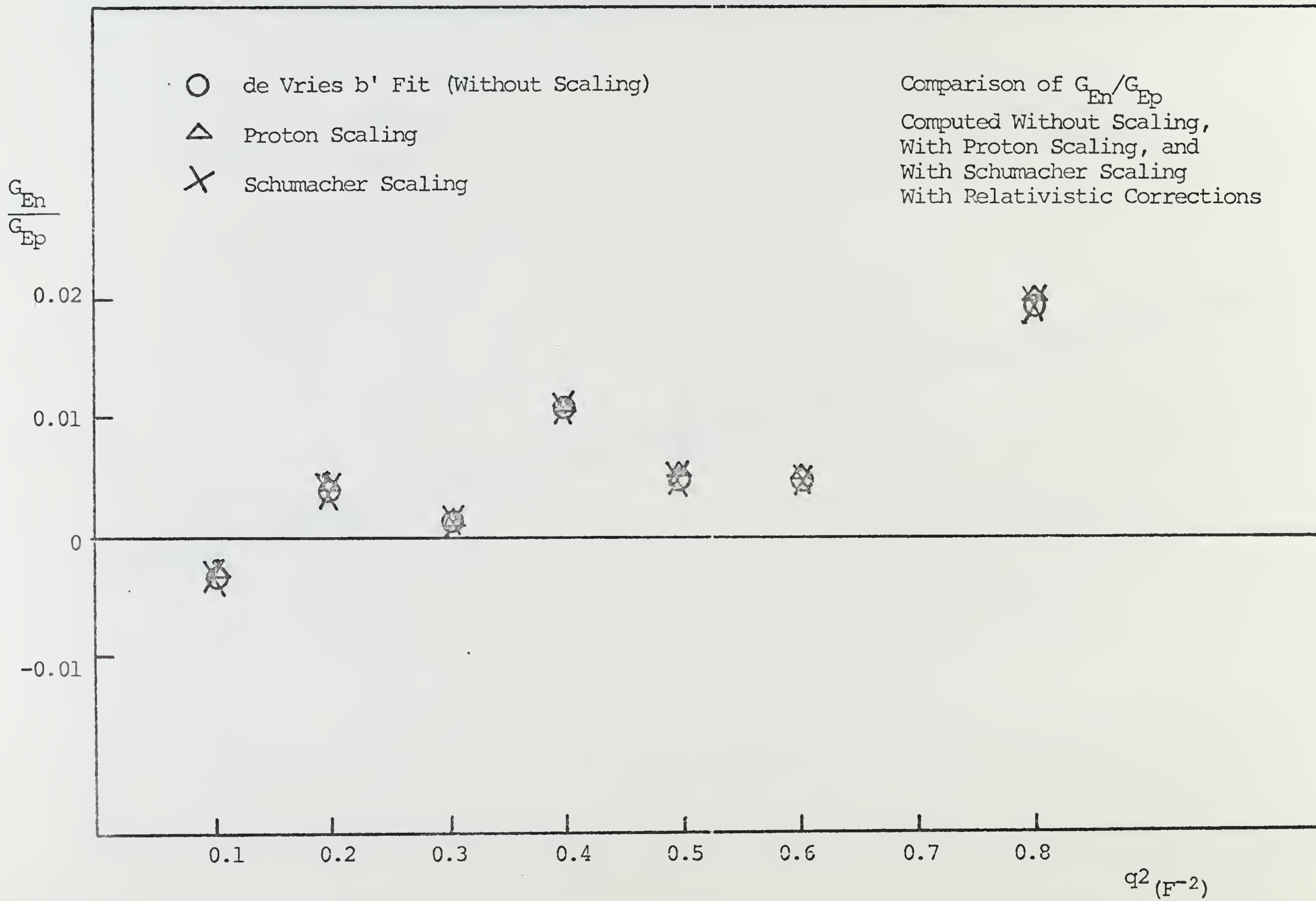
○ de Vries b' Fit (Without Scaling)
△ Proton Scaling
╳ Schumacher Scaling
Comparison of G_{En}/G_{Ep}
Computed Without Scaling,
With Proton Scaling, and
With Schumacher Scaling
With Relativistic Corrections
$\frac{G_{En}}{G_{Ep}}$
0.02
0.01
0
-0.01
0.1
0.2
0.3
0.4
0.5
0.6
0.7
0.8
$q^2\,(F^{-2})$

Figure 5

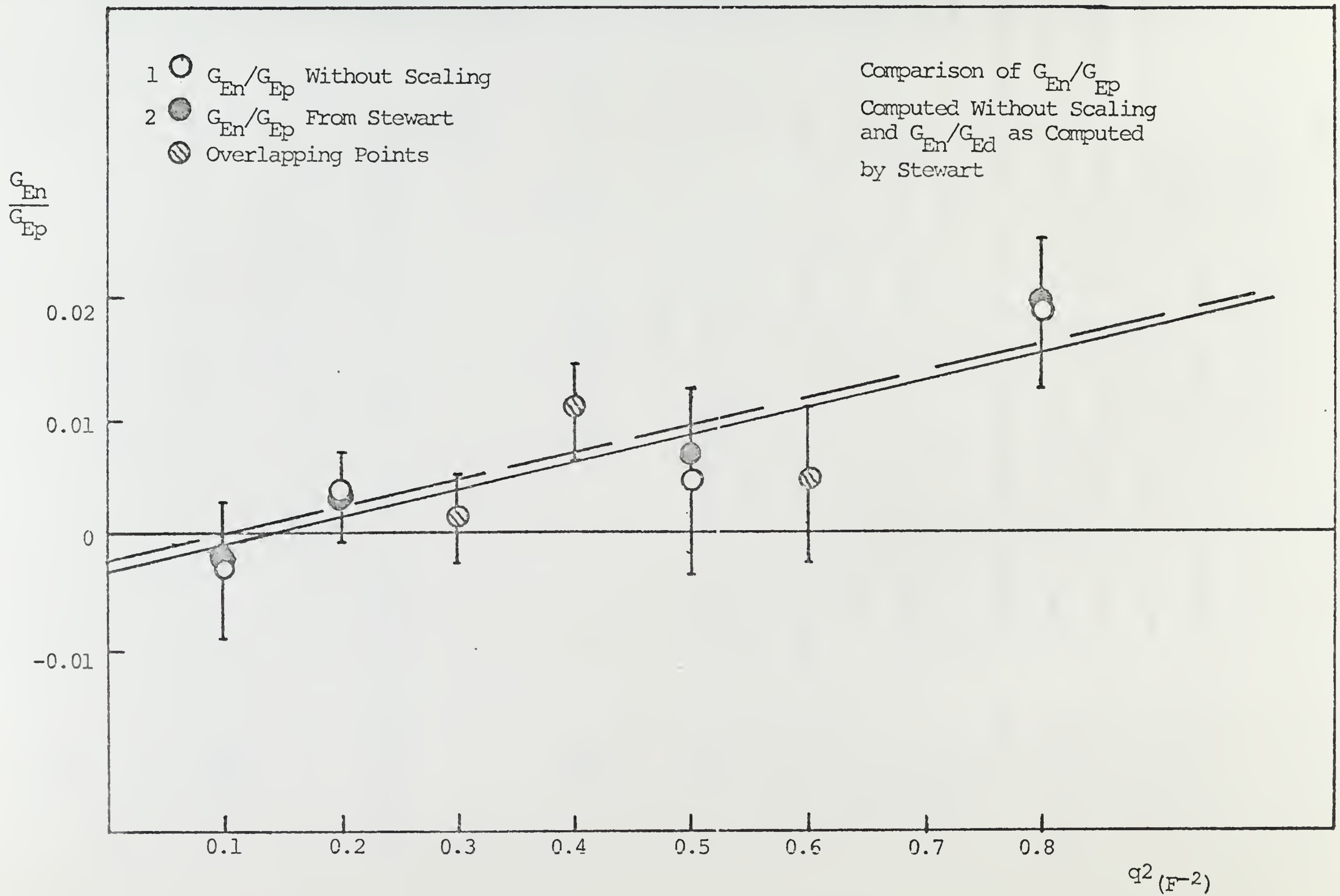
1 G_{En}/G_{Ep} Without Scaling
2 G_{En}/G_{Ep} From Stewart
Overlapping Points
Comparison of G_{En}/G_{Ep} Computed Without Scaling and G_{En}/G_{Ed} as Computed by Stewart
$\frac{G_{En}}{G_{Ep}}$
0.02
0.01
0
-0.01
0.1
0.2
0.3
0.4
0.5
0.6
0.7
0.8
$q^2\ (F^{-2})$

Figure 6

APPENDIX C. STATISTICAL TREATMENT OF DATA

A. WEIGHTED METHOD OF LEAST SQUARES

The principle of least squares can be stated as follows: The most probable value of a quantity is obtained from a set of measurements by choosing the value which will minimize the sum of the squares of the deviations of these measurements. Specifically, if two variables X and Y are known to be related by a linear equation of the form $Y = mX + b$, where m is the slope of the line and b its Y intercept, and if a series of N observations (x_i, y_i) are made in which random errors occur only in the y_i measurements, and the observations are not all samples of the same parent distribution, then the deviations are weighted inversly as the variances of their parent distributions, and Young [17] shows that the quantity to minimize is

$$\Sigma\, w_i d_i^2 = \Sigma\, \frac{d_i^2}{S_i^2} = \Sigma\, w_i (mx_i + b - y_i)^2 \qquad (41)$$

where

$$w_i \,\alpha\, \frac{1}{S_{y_i}^2}$$

and $S_{y_i}^2$ is the variance in y_i [18]. Upon minimizing equation (41) with respect to b and m, the normal equations are

$$\begin{aligned} m\,\Sigma\, w_i x_i + b\,\Sigma\, w_i &= \Sigma\, w_i y_i \\ m\,\Sigma\, w_i x_i^2 + b\,\Sigma\, w_i x_i &= \Sigma\, w_i x_i y_i\ . \end{aligned} \qquad (42)$$

Solving for m and b, it is found that

$$\begin{aligned} m &= M/D \\ b &= B/D \end{aligned} \qquad (43)$$

where

$$M = \begin{vmatrix} \Sigma\ w_i y_i & \Sigma\ w_i \\ \Sigma\ w_i x_i y_i & \Sigma\ w_i x_i \end{vmatrix}$$

$$B = \begin{vmatrix} \Sigma\ w_i x_i & \Sigma\ w_i y_i \\ \Sigma\ w_i x_i^2 & \Sigma\ w_i x_i y_i \end{vmatrix}$$

and

$$D = \begin{vmatrix} \Sigma\ w_i x_i & \Sigma\ w_i \\ \Sigma\ w_i x_i^2 & \Sigma\ w_i x_i \end{vmatrix}$$

The variances in m and b can be calculated by use of the equation

$$S_Q^2 = \Sigma \left(\frac{\partial Q}{\partial y_i}\right)^2 S_{y_i}^2 \tag{44}$$

where S_Q^2 is the variance of the mean of Q, $S_{y_i}^2$ is the variance of the mean of y_i, and so forth. Application of equation (44) to the present situation gives

$$S_b^2 = S_y^2 \ \frac{\Sigma\ w_i x_i^2}{D} \tag{45}$$

and

$$S_m^2 = S_y^2 \ \frac{\Sigma\ w_i}{D}$$

where

$$S_y^2 = w_i \ S_{y_i}^2$$

B. WEIGHTED AVERAGES

If a quantity x is measured by N methods, obtaining values $x_1 \ldots x_N$, which are known to have standard deviations $S_1 \ldots S_N$, then a simple arithmetic average would not give the best value because it would make the x_i equal in weight, while their errors are assumed to be different. A weighted average is then used as

a means of determining the best value. The question is how to assign the correct value of the weight factor w_i to x_i to give the minimum standard deviation in the average value $\bar{x}$. Making a generalization of Beers [18] it is seen that

$$\bar{x} = \frac{\Sigma\, w_i x_i}{\Sigma\, w_i} \qquad (46)$$

and

$$S_{\bar{x}}^2 = \frac{1}{\Sigma \frac{1}{S_i^2}}$$

where

$$w_i \propto \frac{1}{S_i^2}$$

C. PROPAGATION OF ERROR

Young [17] shows that if a quantity Q is to be calculated from several observed quantities x_i and

$$Q = f(x_i)$$

then

$$S_Q^2 = \Sigma \left(\frac{\partial Q}{\partial x_i}\right)^2 S_{x_i}^2 \qquad (47)$$

where S_Q^2 is the variance of the mean of Q, and $S_{x_i}^2$ is the variance of the mean of x_i. Equation (47) can be shown to be true even if different numbers of observation are made on the x_i.

Application of equation (47) gives the variance of the mean for the appropriate functional form of Q.

BIBLIOGRAPHY

1. Rosenbluth, M.N., Phys. Rev., 79, 715 (1950).

2. Yennie, D.R., L'evy, M., and Ravenhall, D.G., Rev. Mod. Phys., 29, 144 (1957).

3. Jannsens, T., and others, Phys. Rev., 142, 922 (1966).

4. Buchanan, C., Ph.D. Thesis, Stanford University, unpublished (1966), and Schumacher, C.R., and Engle, I.M., ANL/HEP, 7032 preprint.

5. Goitein, M., Dunning, J.R., and Wilson, R., Phys. Rev. Ltrs, 18, 1018 (1967).

6. Coward, D.H., and others, Phys. Rev. Ltrs., 20, 292 (1968).

7. Jankus, V.Z., Phys. Rev., 102, 1586 (1956).

8. Glaser, V., and Jaksic, B., Nuovo Cimento, 5, 1197 (1957).

9. Drickey, V.Z., and Hand, L.N., Phys. Rev. Ltrs., 9, 521 (1962).

10. Stewart, J.W., Jr., Elastic Electron Scattering Measurements of the Neutron Charge Form Factor at Very Low Momentum Transfers, Ph.D. Thesis, Naval Postgraduate School (1970).

11. Feshbach, H., and Lomon, E.L., Ann. Phys., 48, 94 (1968).

12. Partovi, F., Ann. Phys. 27, 79 (1964).

13. Sugawara, H., and Von Hippel, F., Phys. Rev., 145, 1331 (1966), and 172, 1764 (1968).

14. Krohn, V.E., and Ringo, G.R., Phys. Rev., 148, 1303 (1966).

15. Adler, R.J., Ph.D. Thesis, Stanford University, unpublished (1965).

16. De Vries, C., and others, Phys. Rev., 134, B848 (1964).

17. Young, H.D., Statistical Treatment of Experimental Data, p. 96-124, McGraw-Hill, 1962.

18. Beers, Y., Introduction to the Theory of Error, 2d Ed., p. 26-43, Addison-Wesley, 1957.

19. Bumiller, F.A., and others, Phys. Rev. Ltrs., 25, 1774 (1970).

INITIAL DISTRIBUTION LIST

		No. Copies
1.	Defense Documentation Center Cameron Station Alexandria, Virginia 22314	2
2.	Library Code 0212 Naval Postgraduate School Monterey, California 93940	2
3.	Professor F.A. Bumiller, 61Bw Department of Physics Naval Postgraduate School Monterey, California 93940	10
4.	Major Joseph H. Brooks 803 Pine Street Oneonta, Alabama 35121	1
5.	Ensign Gregg F. Sessler Boston Post Road Amherst, New Hampshire 03031	1

Unclassified
Security Classification

DOCUMENT CONTROL DATA - R & D

(Security classification of title, body of abstract and indexing annotation must be entered when the overall report is classified)

1 ORIGINATING ACTIVITY (Corporate author) Naval Postgraduate School Monterey, California 93940	2a. REPORT SECURITY CLASSIFICATION Unclassified 2b. GROUP

3 REPORT TITLE

An Investigation of the Influence of Scaling Laws on the Ratio of Neutron-Proton Charge Form Factor Calculations

4 DESCRIPTIVE NOTES (Type of report and inclusive dates)

Master's Thesis; June 1971

5 AUTHOR(S) (First name, middle initial, last name)

Joseph H. Brooks and Gregg F. Sessler

6. REPORT DATE	7a. TOTAL NO. OF PAGES	7b. NO. OF REFS
June 1971	49	19

8a. CONTRACT OR GRANT NO. b. PROJECT NO. c. d.	9a. ORIGINATOR'S REPORT NUMBER(S) 9b. OTHER REPORT NO(S) (Any other numbers that may be assigned this report)

10. DISTRIBUTION STATEMENT

Approved for public release; distribution unlimited.

11. SUPPLEMENTARY NOTES	12. SPONSORING MILITARY ACTIVITY
	Naval Postgraduate School Monterey, California 93940

13. ABSTRACT

An investigation of conventional and broken-symmetry scaling, and their effect on the ratio of the neutron-proton electric form factors, G_{En}/G_{Ep}, was carried out using measurements from elastic electron-deuteron and electron-proton scattering in the range of momentum transfers, q^2, of $0.10 \leq q^2 \leq 0.80\ F^{-2}$, and electron scattering angles of 45° to 120°. Within experimental errors of available data in this range of momentum transfers and angles, it was concluded that both forms of scaling as applied to the deuteron form factor have negigible effect on the ratio G_{En}/G_{Ep}, and the application of either scaling law to the proton form factor results in nearly identical corrections to this ratio, thus allowing no distinction between them, and the agreement of the experimental data with the neutron-electron interaction slope at $q^2 \simeq 0$ is not influenced by the choice of scaling law. A conclusive test for the scaling laws would require an improvement in experimental accuracy by at least an order of magnitude, a technically nearly impossible requirement.

KEY WORDS	LINK A		LINK B		LINK C	
	ROLE	WT	ROLE	WT	ROLE	WT
euteron						
roton						
caling Law						
lectron Scattering						
orm Factors						

128326
Thesis
B80937 Brooks
c.1
An investigation of the influence of scaling laws on the ratio of neutron-proton charge from factor calculations.